2023 13th International Conference on Indoor Positioning and Indoor Navigation (IPIN)

Fingerprint-based fusion of magnetic field data with multiple wireless technologies for indoor mobile robot positioning

Peter Sarcevic
Department of Mechatronics and Automation
University of Szeged
Szeged, Hungary
sarcevic@mk.u-szeged.hu

Dominik Csík
Department of Mechatronics and Automation
University of Szeged
Szeged, Hungary
csikd@mk.u-szeged.hu

Richard Pesti
Department of Mechatronics and Automation
University of Szeged
Szeged, Hungary
pestir@mk.u-szeged.hu

Massimo Stefanoni
Doctoral School of Applied Informatics and Applied Mathematics
Óbuda University
Budapest, Hungary
massimo.stefanoni83@gmail.com

József Sárosi
Department of Mechatronics and Automation
University of Szeged
Szeged, Hungary
sarosi@mk.u-szeged.hu

Ákos Odry
Department of Mechatronics and Automation
University of Szeged
Szeged, Hungary
odrya@mk.u-szeged.hu

***Abstract*—Mobile robot pose information is getting utilized in more and more indoor applications. In this paper, a novel fingerprinting-based positioning method is proposed. The method utilizes magnetic field data together with measurements collected using anchors equipped with multiple wireless technologies. The collected fingerprints are used to train MultiLayer Perceptron (MLP) neural networks, which can later be utilized to estimate the 2D position based on sensor readings in an unknown position. Real measurements collected in a laboratory are used to validate the performance of the method. The measurement database consists of 3D magnetometer measurements and four different parameter types measured between the mobile node and the anchor nodes using multiple wireless technologies. The parameters include Time of Flight (ToF) measurements using Ultra-WideBand (UWB) and Received Signal Strength Indicator (RSSI) measured using WiFi, UWB and 433 MHz frequency band. Various combinations of data were tested in the evaluation process. The obtained results showed that significant improvement, even more than 35%, can be achieved in the positioning performance for most combinations by fusing magnetometer measurements and wireless communication data.**

Keywords—fingerprinting, magnetometer, RSSI, artificial neural network, localization

I. Introduction

Position and orientation information plays a crucial role in many mobile robot applications. Localization of mobile robots is a challenging task, especially in indoor environments. Sensor fusion frameworks estimate the mobile robot's pose based on absolute and relative position information. Relative position can be measured using Inertial Measurement Units (IMU), encoders, etc. Absolute position data can be collected in outdoor applications using GPS, but in indoor environments it does not provide reliable information. Alternative technologies include LiDAR, camera, and wireless communication-based solutions.

Localization methods using wireless signal-based techniques utilize different parameters extracted during the communication of the units, such as Time of Flight (ToF), Time Difference of Flight (TDoF), Angle of Arrival (AoA), Channel State Information (CSI), and Received Signal Strength Indicator (RSSI). In these Wireless Sensor Networks (WSN), the positioning methods applying such parameter types can be split into fingerprint-based and geometric approaches [1]. Both approaches mainly utilize measurements between the node with unknown position and anchor nodes with known position. Geometric approaches include trilateration, multilateration, and triangulation methods. Fingerprinting-based approaches utilize measurements collected in known positions, which are used to train a pattern recognition algorithm. The trained algorithm can be later used to determine the position of an unknown point.

The RSSI is one of the most widely used parameters, which is the signal power received by a receiver. This parameter is usually expressed in decibel milliwatts (dBm). It can be utilized in trilateration-based approaches by converting the parameter value to a distance using an appropriate model, such as the Free Space Path Loss (FSPL) model [2-3]. Another widely used technology in trilateration-based methods is the Ultra-WideBand (UWB) [4], where the distances are computed using ToF measurements. The disadvantage of this technology is its higher cost compared to other technologies, such as WiFi. The fingerprinting-based methods do not require distance information so any parameter type can be directly used as an input.

Vector magnetometers measure the strength of the magnetic field in multiple dimensions. In the case of mobile robots, the Earth's magnetic field enables the use of these sensors as compasses. Magnetic sensors do not provide reliable measurements in indoor environments due to different objects that cause disturbances in the magnetic field [5]. These disturbances can be utilized for indoor localization since each building has its own unique ambient magnetic field.

Geomagnetism-based indoor localization techniques mainly consider smartphone-based human localization [6-7]. These methods mostly utilize a sequence of magnetic field

The work was supported by the National Research, Development, and Innovation Fund of Hungary through project no. 142790 under the FK_22 funding scheme.

measurements alone [8] or fused with other data, such as WiFi [9], CSI [10], Pedestrian Dead Reckoning (PDR) [11], etc. Solutions for the localization of mobile robots based on magnetic sensor measurements were also proposed [12-15]. In [12], a three-axis magnetometer-based technique was proposed using Monte Carlo localization (MCL) for self-localization in one dimension. A deep neural network (DNN)-based approach for indoor positioning method was reported in the literature [13], where the goal was to recognize magnetic sequence patterns. In [14], a localization framework was proposed, which utilized magnetic fingerprints collected with the help of odometry data and a vision-based motion capture system. In [15], a DNN-based method was proposed, where image sequences were built-up based on the time series of changes in the Earth's magnetic field.

Previously, a fingerprinting-based study was proposed where magnetometer data were fused with WiFi RSSI measurements using MultiLayer Perceptron (MLP) feedforward neural networks to provide absolute position information in indoor environment [16]. The results showed that the fused data outperformed the positioning performance of a single technology. Another research showed that utilizing data collected using different wireless technologies can also improve positioning accuracy [17].

In this study, the proposed mobile robot positioning method applies magnetometer measurements together with wireless communication parameters of different technologies. The contributions of the work can be summarized as follows:

- A novel method is proposed for 2D indoor positioning that fuses magnetometer data and measurements of different wireless technologies with the help of MLPs.
- Real measurement data are used to validate the method.
- The performance of the method is evaluated using different combinations of used data.

II. Positioning Method

The proposed fingerprinting-based 2D mobile robot positioning method can be seen in Fig. 1. The method applies

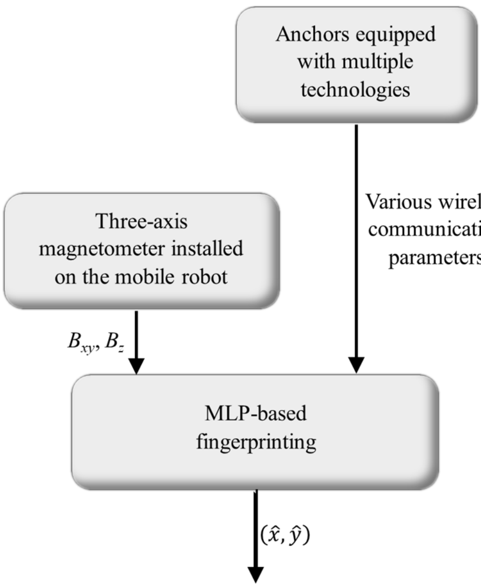

Fig. 1. Proposed fingerprint-based 2D indoor positioning method.

magnetometer data measured on the robot together with different wireless communication parameters measured between the mobile robot and the anchor units with known position.

A. Magnetometer Data

Vector magnetometers provide magnetic field measurements in three dimensions. The measurements of such sensors can be affected by hard and soft iron disturbances [18-19]. Magnetic fields of ferromagnetic materials with permanent magnetism cause hard iron disturbances, which are errors that are additive to Earth's magnetic field. Materials that influence the magnetic field, but do not generate a magnetic field themselves cause soft iron distortions. These errors are not additive. The model for magnetic sensors that are calibrated for deterministic errors can be given using:

$$\boldsymbol{B} = \boldsymbol{A}_{SI}\boldsymbol{m} + \boldsymbol{b}_{HI}, \tag{1}$$

where $\boldsymbol{B} = [B_x \quad B_y \quad B_z]^T$ is the sensor's output, $\boldsymbol{m} = [m_x \quad m_y \quad m_z]^T$ is the Earth's magnetic field, $\boldsymbol{A}_{SI}$ is the 3×3 matrix of soft iron influences, and $\boldsymbol{b}_{HI}$ is the 3×1 vector containing the hard iron errors.

In an indoor space, magnetic field measurements collected in different points can be utilized to construct a fingerprint, which can be used for localization. The measurements in the three axes of the sensor cannot be directly used in the fingerprint without the knowledge of the orientation of the sensor. The magnetic field magnitude can be utilized without information about the orientation. In the case of mobile robots, the degree of freedom decreases to three, i.e., (X, Y, θ), for mobile robots moving on a flat surface. This enables the use of both the Z-axis measurements (B_z) and the magnitude of the magnetic field in the X-Y plane (B_{xy}) in the fingerprint since they are independent from the θ angle. The B_{xy} magnitude can be calculated using (2).

$$B_{xy} = \sqrt{B_x^2 + B_y^2} \tag{2}$$

In [16], the positioning performance of all three versions of magnetic field data were evaluated with and without fusion with RSSI data. The results showed that even magnetic field data alone can provide similar results to RSSI-based results for indoor spaces where the variance of the magnetometer measurements is high. The fusion of the two technologies results in significant improvements compared to the performance achieved using a single technology. Utilizing only magnetometer data, the measurements in the three axes provided the best performance. The use of the 3D magnitude resulted in much lower localization accuracies. The version utilizing B_{xy} and B_z showed promising results since the obtained accuracies were lower than using the measurements in the three axes, but much higher than using the 3D magnitude. In this study, based on the previous considerations, the version based on measurements in the Z-axis and the computed magnitudes in the X-Y plane is applied.

B. Wireless Communication Data

Positioning algorithms in WSNs utilize different parameter types extracted during the communication between the nodes. In an indoor space, different technologies should behave differently due to the differences in signal propagation and path loss. In [17], four parameter types using various technologies were tested in a fingerprinting-based method. The obtained results showed that the localization performance can be improved by the fusion of these technologies. In the proposed method, the different wireless communication parameters are utilized together with the magnetometer measurements.

C. Fingerprinting Algorithm

A multidimensional fingerprint can be constructed using the magnetometer and wireless communication measurements in known positions.

Various pattern matching and pattern recognition techniques can be utilized in fingerprinting-based localization systems. In [17], three widely used algorithms were compared, i.e., the Random Forest (RF), the Weighted K-Nearest Neighbor (WKNN), and the MLP. The best performance of the tested algorithms was achieved using the MLP.

Based on previous results, in the proposed method, three-layer MLPs are applied, which consists of an input layer, an output layer, and one hidden layer. Each used magnetometer or wireless communication parameter is assigned to an input neuron. The two neurons of the output layer provide the $(\hat{x}, \hat{y})$ estimated coordinates. The optimal hidden layer neuron number needs to be found by evaluating different configurations. The used activation function in the hidden layer is the tangent sigmoid, while linear transfer functions are used in the output layer. The collected fingerprint measurements with the corresponding positions can be used to train the MLPs. The trained MLPs can be later used to estimate the position corresponding to measurements in unknown points.

III. Applied Measurement Data

The applied measurement data were collected in the Robotics Laboratory of the Faculty of Engineering, University of Szeged. The enclosing dimensions of the laboratory are 8 m × 12 m. A more detailed description of the used measurement system and the data acquisition process can be found in [16] and [17].

Images of the mobile robot and the measurement environment with a schematic drawing of the laboratory can be seen in Fig. 2. Five anchor nodes with known positions and a mobile robot were utilized. To make the setup more realistic, multiple static objects, such as cabinets and tables, were left in the laboratory. Due to these objects, many points were non-line-of-sight (NLOS) to some anchor nodes.

Both the anchors and the mobile robot were equipped with multiple wireless technologies. The ESP32 NodeMCU was used to provide WiFi RSSI data. A DW1000 UWB module, which is manufactured by Makerfabs, was utilized to provide RSSI and ToF measurements. This module was used only in the case of the first four anchor nodes due to the limitations of the technology. The CC1101 module (later referred to as CC), which is manufactured by Texas Instruments and works in the 433 MHz frequency band, was also used to collect RSSI measurements.

The mobile robot was also equipped with a three-axis digital magnetometer, i.e., a HMC5883L. This magnetic sensor is based on anisotropic magnetoresistive (AMR) technology and can measure in a range of ±810 µT in 12-bit resolution with a maximal sampling rate of 160 Hz. The I2C

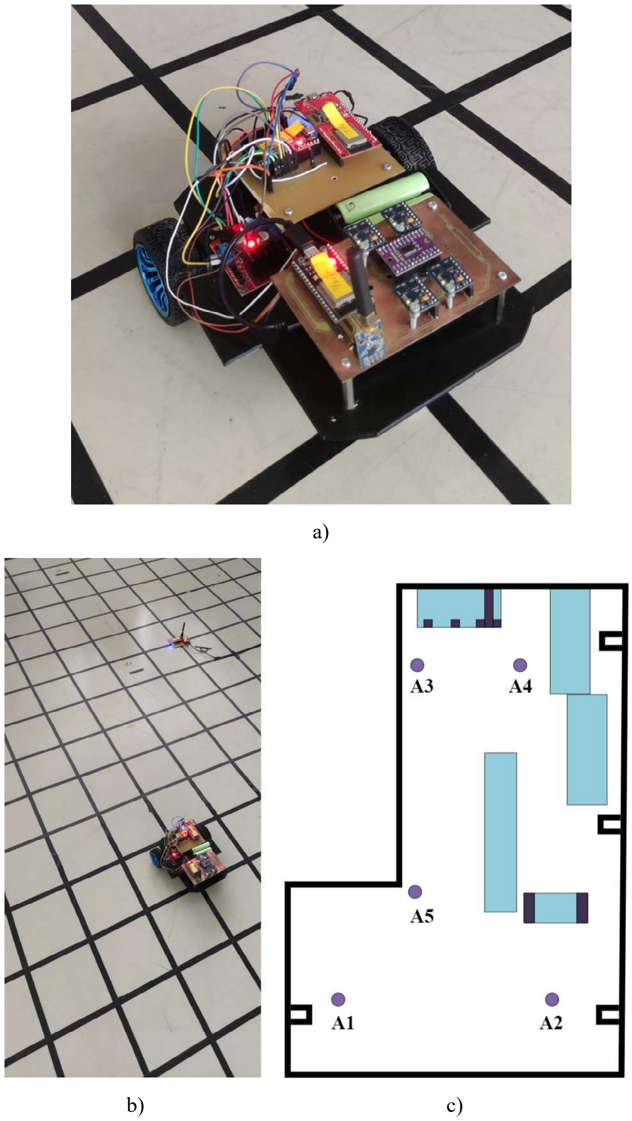

Fig. 2. Measurement setup: a) used mobile robot; b) measurement environment; c) schematic drawing of the laboratory.

interface can be used to configure the sensor and read the measurement data.

The microcontroller of the mobile robot forwarded all measurements to a central unit, where the data were stored.

As it can be seen in Fig. 2, a grid of 20 cm × 20 cm rectangles was created using insulating tape. The robot moved on straight trajectories along the Y-axis and stopped at every intersection defined by the tape to collect measurements. Measurements were collected in a total of 1408 grid points. A further 20 test points were also measured, which were defined by random coordinates and differed from the coordinates of any grid point. In the case of all measurement points, 10 measurements were collected using all technologies. To decrease the effect of noise, the 10 measurements were later averaged.

Fig. 3 shows the heatmaps of UWB ToF and CC RSSI for anchor A1, while the heatmaps of B_{xy} and B_z are given in Fig. 4. The white parts in Fig. 3 and Fig. 4 represent the locations where measurements could not be collected due to obstacles.

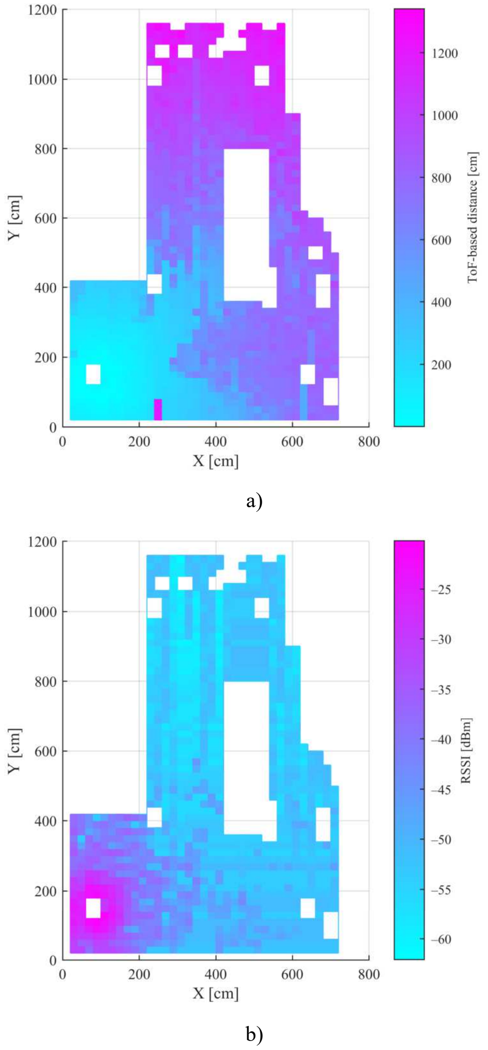

Fig. 3. Fingerprints of wireless data for anchor node A1: a) UWB ToF; b) CC RSSI.

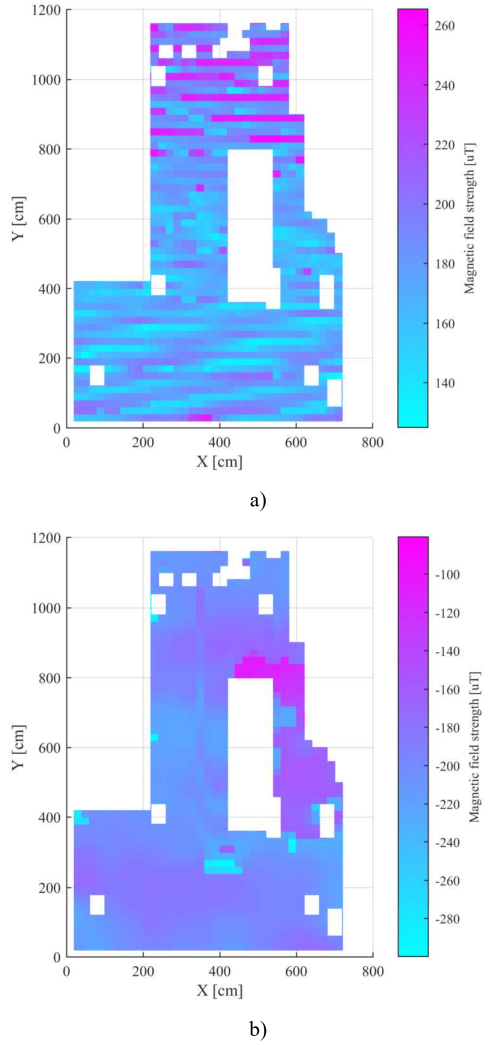

Fig. 4. Fingerprints of magnetometer data: a) B_{xy}; b) B_z.

IV. Experimental Results

The neural networks were trained using the measurement data collected in the grid points. Various datasets were generated based on different combinations of used data types.

The backpropagation algorithm was used for the training of the MLPs. In the training process, 1–100 hidden layer neurons were tested in the case of all datasets to find the optimal configuration. All configurations were tested with 10 initial weight sets since it largely influences the achievable performance of a neural network. In the training process, 70% of the grid points were used as training data, while the remaining 30% as validation data. The results with the lowest error rates were used later in the evaluation process.

The used performance metrics were the Mean Absolute Error (MAE) and the Standard Deviation (STD), which can be calculated using (3) and (4), respectively.

$$\text{MAE} = \frac{1}{M}\sum_{i=1}^{M} E_i, \tag{3}$$

$$\text{STD} = \sqrt{\frac{1}{M-1}\sum_{i=1}^{M}(E_i - \text{MAE})^2}, \tag{4}$$

where M is the number of points, and E_i is the error in the ith point, which can be computed using (5).

$$E_i = \sqrt{(\hat{x}_i - x_i)^2 + (\hat{y}_i - y_i)^2}, \tag{5}$$

where $(\hat{x}_i, \hat{y}_i)$ and (x_i, y_i) are the estimated and real coordinates of the ith point, respectively.

A. Performance Evaluation

Altogether 15 different versions of utilized wireless parameters were tested based on the different combination of the four parameter types. The best obtained results for the different versions are summarized in Table I. Table I contains the achieved lowest MAE and the corresponding STD in the case of training data as well as the MAE and STD results on test data obtained using the same trained MLP. As a comparison, the MLP-based results achieved in [17] are also given in Table I, where only radio communication-based data were fused. The results obtained in [16] using only magnetometer data and the fusion with WiFi RSSI are also given. The results proposed in previous studies are noted in Table I.

TABLE I. ACHIEVED RESULTS USING THE FUSION OF DIFFERENT TECHNOLOGIES

Wireless data	Without magnetometer data [17] (MAE ± STD [cm])		Fusion with of B_{xy} and B_z magnetometer data (MAE ± STD [cm])	
	Training points	***Test points***	***Training points***	***Test points***
none	-	-	228.3 ± 166.7 [16]	232.9 ± 172.6 [16]
CC RSSI	98.8 ± 85.8	175.1 ± 127.7	66.4 ± 59.1	202.8 ± 156.6
UWB ToF	41.7 ± 31.1	84.4 ± 61.0	31.2 ± 26.3	81.5 ± 74.5
WiFi RSSI	174.0 ± 107.0	159.9 ± 115.2	110.2 ± 86.4 [16]	87.6 ± 94.3 [16]
UWB RSSI	125.8 ± 75.2	161.6 ± 102.1	79.1 ± 62.0	158.9 ± 129.8
CC RSSI, UWB ToF	34.1 ± 27.3	125.7 ± 95.3	27.6 ± 21.3	99.0 ± 87.9
CC RSSI, WiFi RSSI	90.0 ± 66.2	144.2 ± 99.5	63.8 ± 56.6	163.8 ± 133.5
CC RSSI, UWB RSSI	70.8 ± 52.1	174.4 ± 119.6	47.7 ± 44.8	197.9 ± 150.2
UWB RSSI, WiFi RSSI	106.2 ± 67.1	148.3 ± 85.6	69.9 ± 58.9	143.0 ± 97.2
UWB RSSI, UWB ToF	37.9 ± 27.5	80.9 ± 62.8	30.45 ± 25.0	84.4 ± 62.4
UWB ToF, WiFi RSSI	44.5 ± 31.9	85.1 ± 62.5	35.15 ± 25.2	77.7 ± 79.2
CC RSSI, UWB ToF, WiFi RSSI	36.9 ± 28.2	131.5 ± 98.6	30.8 ± 23.8	122.5 ± 84.1
CC RSSI, UWB ToF, UWB RSSI	30.2 ± 23.3	117.2 ± 86.4	26.7 ± 29.2	139.1 ± 118.2
CC RSSI, UWB RSSI, WiFi RSSI	63.8 ± 48.4	133.2 ± 82.7	48.4 ± 41.6	122.2 ± 117.3
UWB ToF, UWB RSSI, WiFi RSSI	38.9 ± 28.6	167.0 ± 118.4	31.2 ± 31.0	92.8 ± 80.3
CC RSSI, UWB ToF, WiFi RSSI, UWB RSSI	31.7 ± 25.3	132.2 ± 87.9	27.7 ± 26.3	145.8 ± 120.3

Analyzing the achieved results given in Table I, it can be observed that the fusion of wireless communication data with magnetometer readings can significantly improve the positioning performance compared to the results reported in [17]. In the case of training data, the MAE improved for all combinations by magnetometer augmentation. The improvement reached even more than 35%. In the case of test points, some versions provided lower accuracies with magnetic sensor data than without it. These versions were mostly the combinations where CC RSSI data were utilized. The most significant improvement, where the MAE for test points decreased from 167.0 cm to 92.8 cm, was obtained with the combination utilizing both WiFi RSSI and the two UWB parameters.

In [16], the magnetometer measurements were fused with WiFi RSSI fingerprints, and the reported errors were 110.2 ± 86.4 cm and 87.6 ± 94.3 cm for training and test points, respectively. Observing the obtained results where only a single wireless data type was utilized, the UWB ToF parameter significantly outperformed the other three parameters. Using this parameter, by adding magnetometer data, the errors decreased from 41.7 ± 31.1 cm to 31.2 ± 26.3 cm and from 84.4 ± 61.0 cm to 81.5 ± 74.5 cm for training and test data, respectively. These errors are significantly lower than the reported results in [16]. In the case of the remaining two parameters, i.e., UWB RSSI and CC RSSI, the fusion with magnetometer fingerprints improved the MAE by more than 30% on training data.

The fusion of multiple wireless data types with magnetometer measurements further improved the results. Fusing other wireless data with the UWB ToF, which provided the best results from the four tested parameter types, does not significantly improve the results. In the case of training points, multiple versions provided lower error rates than using only the UWB ToF data. The best results were obtained using the fusion of CC RSSI, UWB ToF, and UWB RSSI together with the magnetic sensor data, where the MAE was 26.7 cm. The fusion of magnetometer data with different wireless data types has a significant effect when RSSI parameters are utilized together. The fusion of the three RSSI parameters with magnetometer fingerprints provided 48.4 cm MAE on training data, while the results were 66.4 cm, 110.2 cm, and 79.1 cm using only CC, WiFi, and UWB technology, respectively. The obtained errors for the fusion of the three RSSI parameters without magnetometer measurements were 63.8 ± 48.4 cm [17]. The lowest errors on test points, i.e., 77.7 ± 79.2 cm, were obtained by fusing UWB ToF and WiFi RSSI data.

The obtained results showed that the tested hidden layer neuron numbers of the MLPs were sufficient since convergence was achieved in the case of all datasets.

V. CONCLUSION

In this paper, a novel fingerprint-based indoor 2D positioning method was proposed for mobile robots. The method fuses magnetometers data and measurements of multiple wireless technologies using MLP neural networks.

Real measurement data collected in a laboratory were used to validate the method. The measurement database consists of grid points applied for training and test points used for validation of the fingerprinting algorithm. The applied magnetic field information is usable without the knowledge of the orientation in the case of robots moving on a flat surface. Four different wireless communication parameter types were tested, which were extracted using three different technologies. To explore the performance of the proposed method, various combinations of used data were tested.

The results showed that significant improvement can be achieved by fusing the magnetometer measurements with wireless communication parameters. In the case of grid points, which were used as training data, the improvements reached even above 35%, while for test points improvements were obtained in most versions of used data.

Future research goals include the testing of the contribution of different anchor nodes. The effect of the fusion of different technologies in different zones of the given indoor space should also be investigated. Further goals include the implementation of the positioning method into a sensor fusion framework. The orientation estimation of the sensor fusion framework could also enable the usage of the magnetometer measurements in the three sensor axes in the proposed fingerprinting method.

REFERENCES

[1] N. Singh, S. Choe, and R. Punmiya, "Machine Learning Based Indoor Localization Using Wi-Fi RSSI Fingerprints: An Overview," IEEE Access, vol. 9, pp. 127150–127174, 2021.

[2] B. Yang, L. Guo, R. Guo, M. Zhao, and T. Zhao, "Machine Learning Based Indoor Localization Using Wi-Fi RSSI Fingerprints: An Overview," IEEE Sens. J., vol. 20, pp. 8164–8172, 2020.

[3] D. Csík, P. Sarcevic, R. Pesti, and Á. Odry, "Comparison of different radio communication-based technologies for indoor localization using trilateration," in Proc. of IEEE International Symposium on Applied Computational Intelligence and Informatics (SACI), 2023, pp. 487–492.

[4] F. Mazhar, M. G. Khan, and B. Sällberg, "Precise Indoor Positioning Using UWB: A Review of Methods, Algorithms and Implementations," Wirel. Pers. Commun., vol. 97, pp. pages 4467–4491, 2017.

[5] B. Li, T. Gallagher, A. G. Dempster, C. Rizos, "Comparison of different radio communication-based technologies for indoor localization using trilateration," in Proc. of International Conference on Indoor Positioning and Indoor Navigation (IPIN), 2012, pp. 1–9.

[6] S. He and K.G. Shin, "Geomagnetism for Smartphone-Based Indoor Localization: Challenges, Advances, and Comparisons," ACM Comput. Surv., vol. 50, 97, 2018.

[7] G. Ouyang and K. Abed-Meraim, "A Survey of Magnetic-Field-Based Indoor Localization," Electronics, vol. 11, 864, 2022.

[8] I. Ashraf, M. Kang, S. Hur, and Y. Park, "MINLOC:Magnetic Field Patterns-Based Indoor Localization Using Convolutional Neural Networks," IEEE Access, vol. 8, pp. 66213–66227, 2020.

[9] Y. Li, Z. He, J. Nielsen, and G. Lachapelle, "Using Wi-Fi/Magnetometers for Indoor Location and Personal Navigation," in Proc. of International Conference on Indoor Positioning and Indoor Navigation (IPIN), 2015, pp. 1–7.

[10] X. Huang, S. Guo, Y. Wu, and Y. Yang, "A fine-grained indoor fingerprinting localization based on magnetic field strength and channel state information," Pervasive Mob. Comput., vol. 41, pp. 150–165, 2017.

[11] G. Wang, X. Wang, J. Nie, and L. Lin, "Magnetic-Based Indoor Localization Using Smartphone via a Fusion Algorithm," IEEE Sens. J., vol. 19, pp. 6477–6485, 2019.

[12] J. Haverinen and A. Kemppainen, "Global indoor self-localization based on the ambient magnetic field," Rob. Auton. Syst., vol. 57, pp. 1028–1035, 2009.

[13] N. Lee, S. Ahn, and D. Han, "AMID: Accurate Magnetic Indoor Localization Using Deep Learning," Sensors, vol. 18, 1598, 2018.

[14] M. Frassl, M. Angermann, M. Lichtenstern, P. Robertson, B. J. Julian, and M. Doniec, "Magnetic Maps of Indoor Environments for Precise Localization of Legged and Non-legged Locomotion," in Proc. of IEEE IEEE/RSJ International Conference on Intelligent Robots and Systems (IROS), 2013, pp. 913–920.

[15] L. Antsfeld and B. Chidlovskii, "Magnetic Field Sensing for Pedestrian and Robot Indoor Positioning," in Proc. of International Conference on Indoor Positioning and Indoor Navigation (IPIN), 2021, pp. 1–8.

[16] P. Sarcevic, D. Csik, and A. Odry, "Indoor 2D Positioning Method for Mobile Robots Based on the Fusion of RSSI and Magnetometer Fingerprints," Sensors, vol. 23, 1855, 2023.

[17] D. Csik, Á. Odry, and P. Sarcevic, "Fingerprinting-Based Indoor Positioning Using Data Fusion of Different Radiocommunication-Based Technologies," Machines, vol. 11, 302, 2023.

[18] G. Secer and B. Barshan, "Improvements in deterministic error modeling and calibration of inertial sensors and magnetometers," Sens. Actuator A Phys., vol. 247, pp. 522–538, 2016.

[19] N. Hadjigeorgiou, K. Asimakopoulos, K. Papafotis, and P.P.Sotiriadis, "Vector Magnetic Field Sensors: Operating Principles, Calibration, and Applications," IEEE Sens. J., vol. 21, pp. 12531–12544, 2021.